James Webb Space Telescope Sunshield: Challenges in Analysis of Gossamer Structures

Ryan A. Fellini and Yury L. Kropp
Northrop Grumman Space Technology

The sunshield of the James Webb Space Telescope will be one of the largest deployable structures ever constructed. Comprising multiple layers of ultrathin membrane material (a gossamer structure), the sunshield will dissipate internal spacecraft heat and shield the optics from solar radiation—both critical to the performance of the observatory. One of the most important aspects of the structural analysis is the accurate, reliable on-orbit prediction of the global shape, along with the determination of any significant local wrinkling. Robust analytical procedures have been developed at Northrop Grumman Space Technology, employing geometric, nonlinear, large-deflection finite element analysis. A test program of incremental complexity has been initiated to validate those methodologies.

This article reviews existing analyses in the gossamer structures community, the challenges in the analysis and design of such structures, and the analytical tools developed thus far. The results from two completed correlation tests and an overview of the lessons learned are presented, showing significant progress in understanding the physics of gossamer structures. The tools have been implemented to optimize the shape of the sunshield and continue to evolve through testing of the model-to-hardware correlation.

Introduction

The James Webb Space Telescope (JWST), under development to succeed the Hubble Space Telescope, will be the astronomical community's premier space-based observatory when launched sometime in the next decade. The observatory is being integrated by Northrop Grumman Space Technology under contract to the National Aeronautics and Space Administration's Goddard Space Flight Center. The primary objective of the JWST is to search for *first light*—light that was emitted following the Big Bang. To do so, the observatory must use a telescope that captures light within the infrared band. For protection against stray light emissions, the entire observatory must remain in a cryogenic state and be shielded from any direct or indirect (reflected) sunlight emissions.

The JWST's sunshield will be one of the largest space deployables ever constructed. It will be composed of multiple layers of ultrathin membrane material, creating a *gossamer* structure. The sunshield will protect the scientific equipment and optical systems from infrared emissions, necessary in order for the observatory to detect faint infrared emissions within the wavelength range of 0.6 to 28 μm. Additionally, the sunshield will dissipate heat from within the spacecraft's bus toward outer space, vital for maintaining a cryogenic environment. Both protective functions are critical to the performance of the observatory and depend on achieving a well-defined shape for the sunshield while on orbit. Accurate prediction of the shape involves both the global structure and the identification and control of wrinkling to very tight specifications. Northrop Grumman

Space Technology has developed and is using robust geometric, nonlinear, large-deflection finite-element analysis procedures to predict structural performance on orbit.

The JWST will be placed in an L2 Lagrange stationary-point orbit 1.5 million kilometers (932,000 miles) from Earth and 150 million kilometers (93.2 million miles) from the Sun. At L2, Earth, Sun, and spacecraft line up, minimizing thermal disturbances from Earth, Sun, and Moon [1]. The combined gravitational pull helps to maintain a stable orbit, requiring little rocket thrust to keep the spacecraft in position.

Figure 1 depicts the optical telescope element, which is the heart of the observatory and includes the primary and secondary mirrors. The primary mirror is a 6.5-m (21.3-ft) diameter beryllium reflector comprising18 hexagonal mirror segments. The secondary mirror and two segments of the primary mirror are folded into a stowed position for launch. Figure 1 shows the sunshield in its fully deployed configuration, isolating the telescope at the cold side of the observatory.

Figure 2 shows the observatory from the side of the spacecraft oriented toward the Sun. The spacecraft's bus, solar arrays, and communications antenna are all visible in this hot-side view of the observatory. Enclosed behind the primary mirror is the Integrated Science Instrument Module (ISIM), which contains the fine-guidance sensors, near-infrared camera, near-infrared spectrograph, and mid-infrared instrument. The ISIM electronics compartment is at the bottom of the ISIM. Directly below the ISIM module is the ISIM electronics compartment. In addition to shielding the observatory from sunlight, the sunshield's cold side must avoid backreflecting generated heat to the scientific equipment or the telescope.

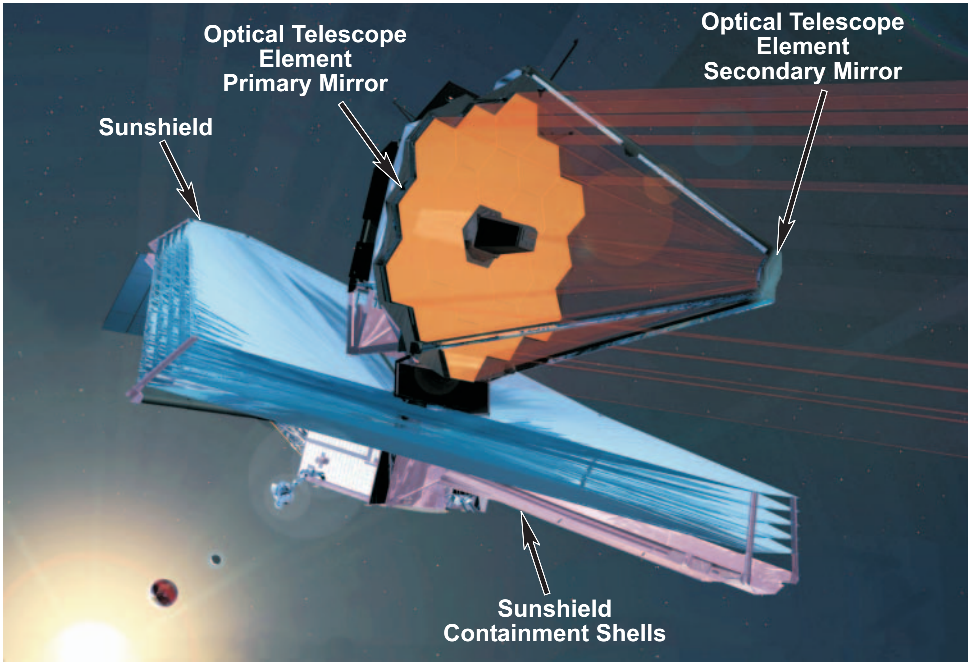

Figure 1. Deployed observatory, front view: Optical telescope element

The JWST's sunshield, about the size of a tennis court, uses five layers of ultrathin membrane constructed from DuPont™ Kapton® E [2]. The first layer, at the hot side, is 2.0 mil (50.8 µm) thick. The remaining four layers are each 1.0 mil (25.4 µm) thick, similar in thickness to a human hair. The membranes use a vapor-deposited aluminum coating in order to produce a highly reflective surface and can sustain a 300 K (300°C, 540°F) temperature drop. Z-folded at launch, the sunshield will be signaled to begin deploying two days into launch, as the spacecraft heads toward its orbit. Figure 3 shows the various stages of sunshield deployment.

In addition to meeting the complex requirements of the sunshield subsystem, one of the most critical aspects of the structural analysis is the accurate, reliable on-orbit prediction of the global shape, along with determination of any significant local wrinkling. Further, the slopes of wrinkles at critical locations must not exceed specified magnitudes, in order to ensure minimization of detrimental thermal effects.

Historically, membranes have been designed to induce a biaxial-tension stress state, thus guaranteeing that wrinkles do not form. The large-scale geometry of the JWST sunshield, along with its complex design features, may hinder such a biaxial stress state. Therefore, the ability to accurately predict the response of the membrane becomes critical to mission success. This article addresses the analytical problems involved in meeting those objectives and looks ahead to the challenges remaining in manufacturing the sunshield.

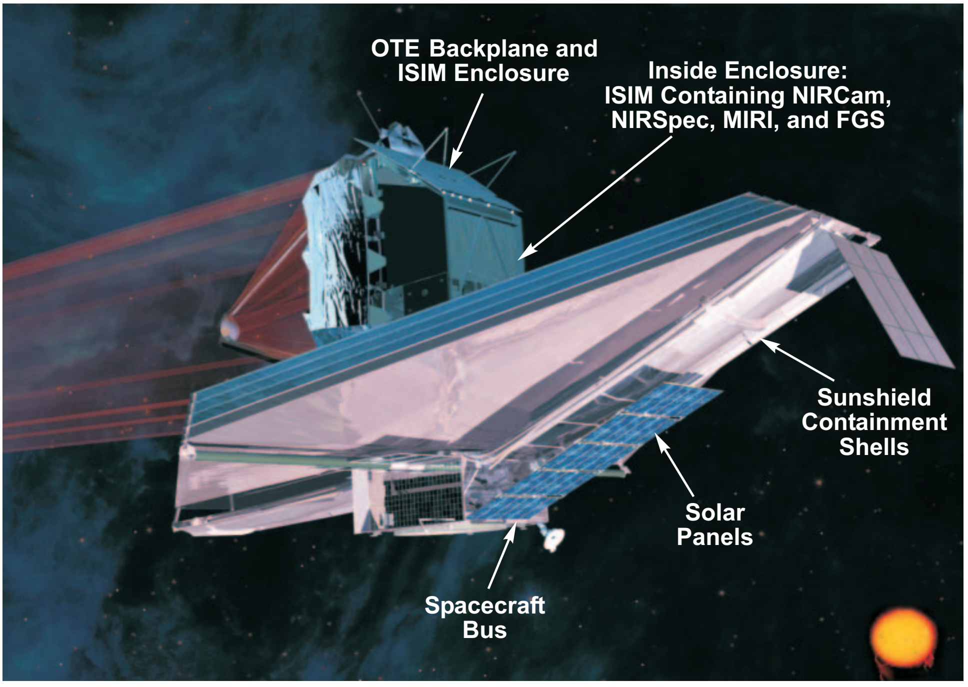

Note: FGS = Fine guidance sensor
ISIM = Integrated Science Instrument Module
MIRI = Mid-infrared instrument
NIRCam = Near-infrared camera
NIRSpec = Near-infrared spectrometer
OTE = Optical telescope element

Figure 2. Deployed observatory, back view: Bus, solar arrays, communications antenna, and Integrated Science Instrument Module

a. Stowed b. Deploying c. Fully deployed

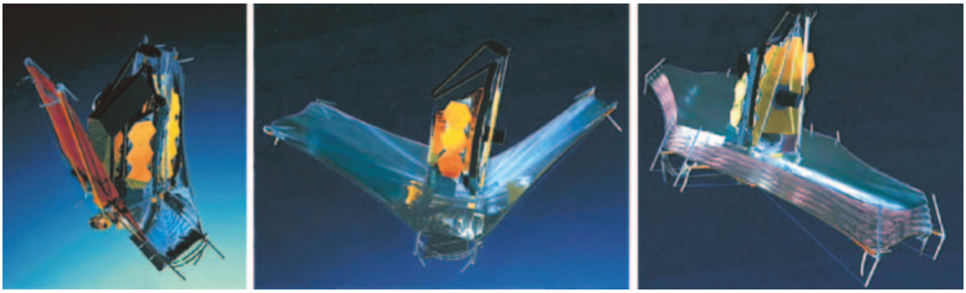

Figure 3. Sunshield deployment

Previous Work on Gossamer Structures

A tension-only structure is a physical artifact whose elements carry only tensile loads with no bending or compression. Examples include suspension bridges, pressure vessels, and bicycle wheels. Modern analytical understanding of such structures began in the late 19th century with the Russian engineer Vladimir Shukhov, notable for his work in hyperboloid, shell, and tension structures. A gossamer structure is a subset of such structures, in which a membrane is used as the primary structural component. Common examples include inflatable structures, such as hot-air balloons, dirigible (semirigid) air ships, and standing canopies (or awnings), as used in the Denver International Airport (Figure 4).

The benefit of using gossamer structures in spacecraft is primarily mass efficiency, allowing the spacecraft designer to efficiently implement a reflector, sunshield, or other large structure. One application of particular interest has been the solar sail, which is a propulsion mechanism driven by the pressure of photons emitted from the Sun. Attempts have been made to fly gossamer structures in space, including a 25-m Mylar® polyester film mirror and a solar sail technology demonstration. Unfortunately, the mirror failed to deploy and the sail spacecraft was lost during launch. Concepts are being studied now in which gossamers are used to construct large optical elements, an entire space station, or star shades that orbit in front of telescopes in order to identify planets—such as in the proposed New Worlds Observer.

Although gossamer structures are very attractive from an optimal design standpoint—they offer an excellent mass-to-load ratio—their incorporation into mainstream engineering structures has been slow because of the substantial challenges in the analysis of such structures. Until recently, only simple closed-form solutions existed, which limited options for designers. Those solutions typically addressed cases of planar structures or bodies of revolution, such as pressure vessels.

The methods developed to date all suffer from the fundamental limitation that they are applicable to planar structures only. The sole method currently capable of solving general three-dimensional gossamer structures is to employ a nonlinear, large-deflection finite element model (FEM) analysis. However, early attempts to apply large-deflection FEM analysis to ultrathin structures were unsuccessful. Designers faced severe convergence problems due to the ill conditioning of the stiffness matrix—i.e., the case in which the out-of-plane stiffness is orders of magnitude lower than the in-plane stiffness. Eventually, the

Photo courtesy of Denver Metro Convention & Visitors Bureau

Figure 4. Modern gossamer structure: Denver International Airport

problems were solved by either preloading a structure, as in the case of two-dimensional structures—or, more generally, using some sort of solution stabilization schemes [3,4]. Yet another approach is to employ an explicit dynamic solver such as ABAQUS® or DYNA3D.

The stabilization scheme of the ABAQUS implicit solver—the program considered best suited for analysis of unstable structures—is essentially a pseudodynamic process whereby damping is carefully selected to prevent numerical instability. Finding a solution via that process remains a significant challenge. Unless damping is completely removed, the accuracy of the solution cannot be ensured. In an explicit dynamic analysis, no solution iterations are required, because the subsequent step is predicted based on the state of the current step. To guarantee accuracy, however, very small steps are required, making the process computationally intensive. Also, to predict shorter wavelengths, fine-grid models may be required, further compounding the problem. Consequently, the accuracy of the solution remains a question and the corresponding deformed shape a problem, since equilibrium at the nodes is never satisfied for the current load step.

The analysis approach used on JWST is based on the robust nonlinear features of MSC.Nastran®, combining it with an enhanced solution strategy and thus enabling it to overcome a potential ill conditioning of the stiffness matrix. Northrop Grumman's approach combines the best features of ABAQUS and MSC.Nastran, making it ideally suited for the solution of gossamer structures. Results generated using the Northrop Grumman approach on the JWST sunshield are discussed in the following section.

For a more general review of the advancements in manufacturing, measurement, and analysis of gossamer structures, refer to the books edited by Jenkins [5,6].

Analysis of James Webb Space Telescope Sunshield

Unique challenges have been encountered during the design, analysis, and verification of the JWST sunshield—all due to the complex operational and environmental requirements, coupled with geometrical and material constraints. The multilayer, complexly curved, somewhat irregular geometry is a radical departure from previous gossamer structures.

The JWST sunshield's primary function is to prevent the Sun's rays from reaching the telescope mirrors and instruments, thereby keeping them at cryogenic temperatures. Another important sunshield function is to radiate the heat generated by the spacecraft bus toward outer space. The five layers are configured to fan out from the bus with dihedral angles that ensure no thermal radiation is trapped within layers. Also, no contact is permitted between layers or between the sunshield layers and the spacecraft hardware. Any contact between the upper layer and the optical telescope element is strictly prohibited.

One challenge in sunshield design is the need to minimize wrinkles. If the sunshield in its fully tensioned state develops deep wrinkles, the layers might come into contact, thereby violating the thermal requirements. An additional constraint imposed on the cold layer requires that no more than 2% of the heat rays emitted by the ISIM electronics compartment reflect back into the ISIM module. An analytical ray-trace procedure was developed and executed to calculate the reflected heat. In that process, the heat-ray distribution is discretized and individual rays are followed as they reflect off the finite elements of the sunshield.

The analysis has shown that the presence of even small wrinkles oriented in a critical direction may dramatically increase the amount of heat reaching the equipment. It is therefore critical to be able to predict the shape of the smallest details in the tensioned sunshield, including the wrinkles. Unfortunately, the great size of the sunshield relative to the size of potential wrinkles renders the FEM extremely computation intensive. Nevertheless, FEM analysis has been conducted incrementally, executing ever-finer FEMs and comparing results to determine if the process had converged. The analysis of the nominal shape converged with an element size of 2 in. (5.08 cm). Figure 5 illustrates a full five-layer FEM of the sunshield.

Shape Optimization. Because the sunshield design combines dynamics, materials, structures, and thermal analyses, the final design is necessarily a compromise among the requirements imposed by all of those disciplines. Initially, the sunshield was configured as a collection of planar faces because it is believed to be thermally optimal. The initial shape

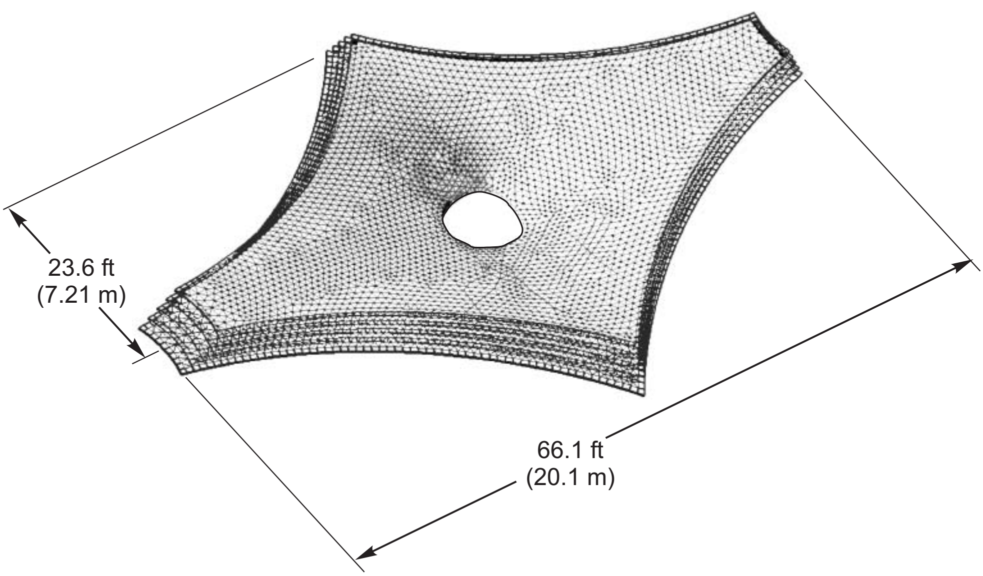

Figure 5. Full five-layer finite element model of James Webb Space Telescope sunshield

is denoted as the design or the computer-aided design (CAD) shape. However, analysis has demonstrated the CAD shape to be unsustainable without additional restraints.

In the final design process, the structural analyst calculates the shape under load, and the other disciplines will determine whether the shape is acceptable. In calculating the deformed shape, the objective should be a final shape that is fully tensioned, devoid of wrinkles, and as stiff as the constituent material. Such surfaces, known in physics and mathematics as membrane shapes, are a subset of minimal surfaces that are nearly impossible to calculate in closed form (except a few idealized shapes, such as a soap bubble or catenoid surface).

Significant progress was made when a FEM-based methodology, implemented using Northrop Grumman's enhanced FEM tools, was formulated to calculate membrane shapes under any edge conditions. To the authors' knowledge, no similar methodology has been reported in the literature. The algorithm to derive the membrane shape is based on an iterative solution in which the CAD shape is used as a starting point for the subsequent shape calculation. By performing that computationally intensive analysis, we were able to arrive at a completely wrinkle-free sunshield. Further, the maximum deflection due to the tensioning of the layers could be reduced to 0.020 in. (0.508 mm).

Figures 6 and 7 show examples of pre- and postoptimization, respectively. The first tensioned membrane (Figure 6) is based on geometry directly from the subsystem CAD geometry (for an older version of the sunshield). Such a shape is not optimal under tension and shows significant wrinkling. The second tensioned membrane (Figure 7) is analyzed after the membrane shape optimization; wrinkling in this complex shape is all but nonexistent.

Performance Analysis. When on orbit, the sunshield is designed to withstand the effects of solar radiation, including solar pressure. Although infinitesimal over a small area, the cumulative effect of that pressure can become significant when acting on large surfaces, as in a solar sail. To balance the moment due to the solar pressure, the forward half of the sunshield will be raised or lowered before launch, creating a pitch-change condition. That condition constitutes another complexity for the structural analysis, as the membranes

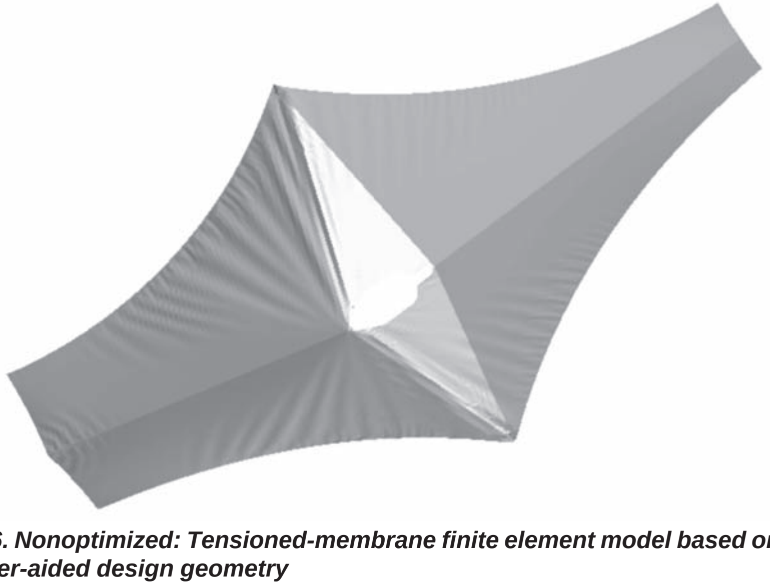

Figure 6. Nonoptimized: Tensioned-membrane finite element model based on computer-aided design geometry

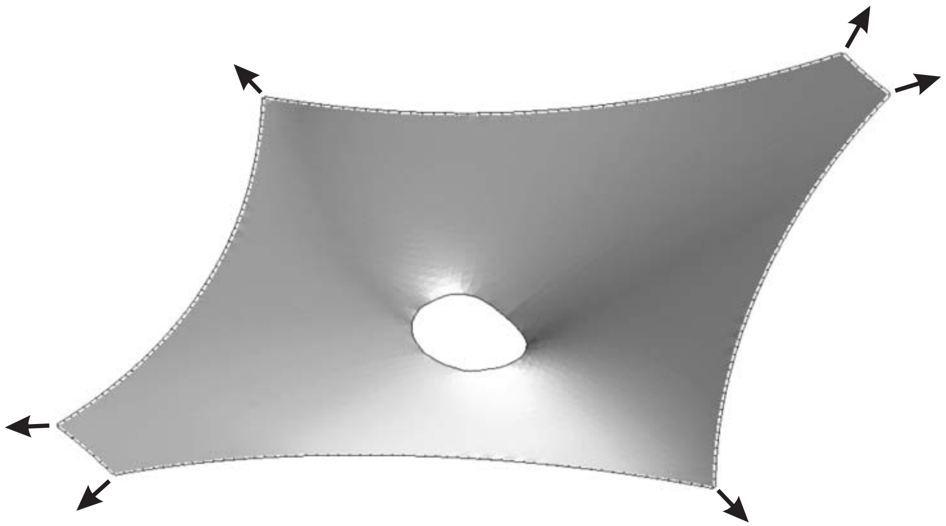

Figure 7. Optimized: Tensioned-membrane finite element model based on membrane shape

analyzed in the nominal 0-deg configuration will now have to be rotated ±2.0 deg, resulting in vertical adjustments of up to 11.6 in. (29.5 cm). Such a pitch change is very traumatic for the already delicately balanced membranes, so convergence is not achieved easily. The result of such an analysis, for a positive 2.0-deg pitch change, is shown in Figure 8. Note the presence of deep wrinkles.

Further computational complexity results from the sunshield's extremely thin layers of Kapton, which will experience high temperature gradients when exposed to the Sun. Since the material exhibits a sizable coefficient of thermal expansion, wrinkles might form to absorb the thermally induced strains. Currently, the sunshield is designed to be tensioned with 15 psi (103.4 kPa) of average stress, which is not enough to overpower thermal stresses. However, that value was selected after carefully balancing the need to minimize material imperfections, such as creases, while maintaining the membrane stress below a level likely to cause any tears to propagate.

Likewise, the hardware support structure must not be overloaded. Higher membrane tension would also increase the natural vibration frequency, although that increase was not shown to be a design driver. FEM analyses were executed to evaluate the deformed shape of the sunshield under various thermal conditions and to verify that the shape requirements were not violated. Figure 9 presents results from a thermal analysis.

The thermal load is applied to the cold layer that has already been subjected to a positive pitch change. The thermal load aids in pulling out the wrinkles due to pitch change; however, wrinkles then occur near the center of the sunshield. The cold layer is subjected to the most benign temperature gradient. In both the pitch-change and thermal calculations, the analysis methodology allows the prediction of the on-orbit shape and verification that performance requirements have been met, helping to ensure mission success.

Analysis and Verification Flow. We have devised a process flow to verify the sunshield's membrane readiness for launch. Figure 10 presents an overview of the full procedure from design to final manufacture of the flight article. Once the optimized membrane shape has been obtained, the sunshield's on-orbit shape is predicted and checked for interferences.

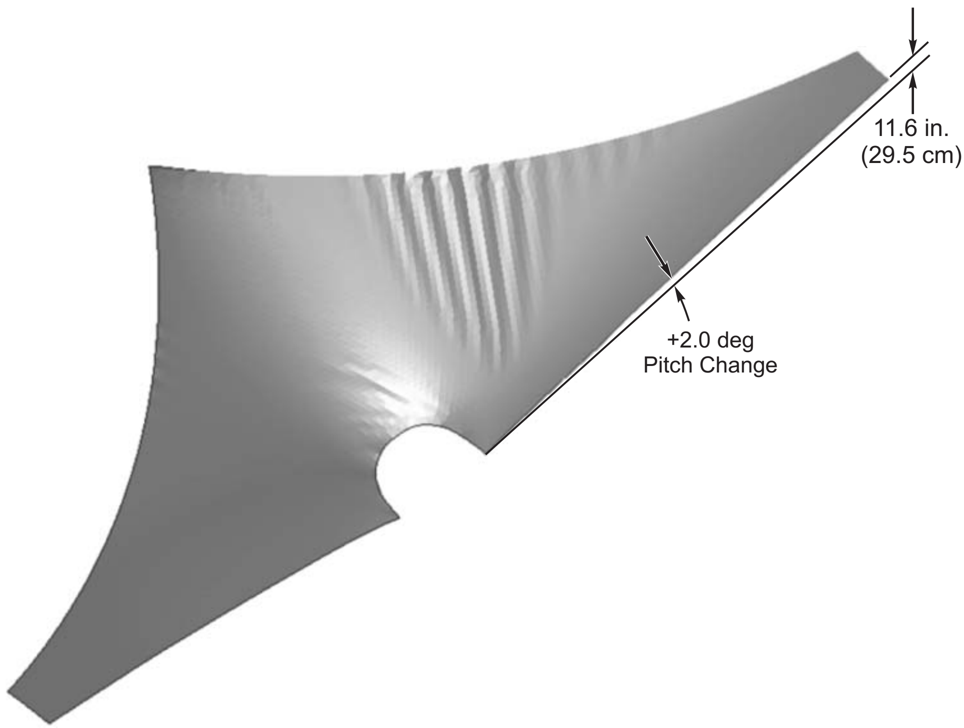

Figure 8. Forward-section positive pitch change of James Webb Space Telescope sunshield

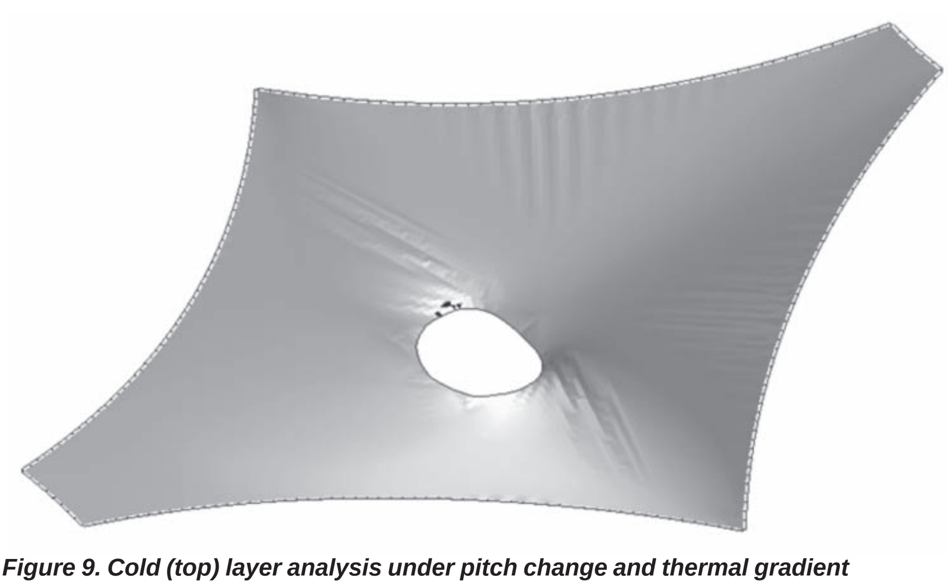

Figure 9. Cold (top) layer analysis under pitch change and thermal gradient

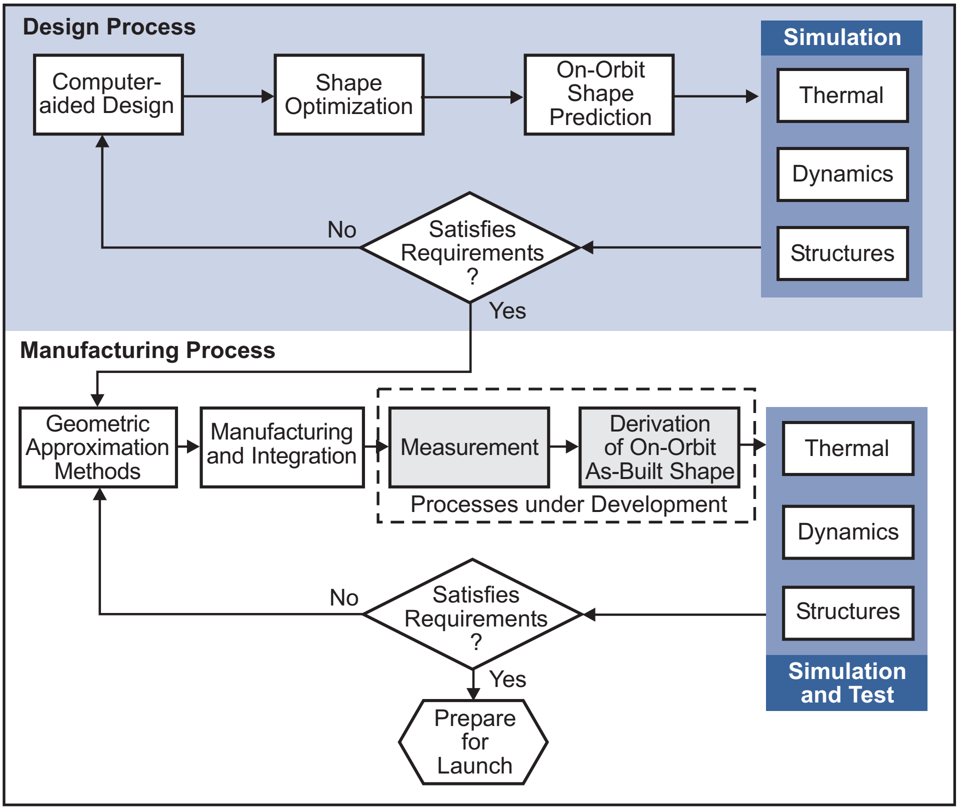

Figure 10. Overview of James Webb Space Telescope sunshield analysis process

Then the ray-trace and thermal analyses are executed. Subsequently, the sunshield simulation model is subjected to the maximum pitch-change operation and the performance verification process is repeated.

This process was executed on the latest JWST configuration and the sunshield performance evaluated. Although the analysis of sunshield membranes is complex and computationally intensive, the structure team at JWST has overcome the many technical challenges and successfully verified the performance of the first design iteration of the sunshield.

However, the process described so far pertains only to ideally constructed sunshields. During design, we learned that strategies must be devised to deal with real-life manufacturing conditions. Consequently, we are now devising procedures for measurement and the determination of the as-built shape. Shown as gray-filled boxes in the process flow, they are beyond the scope of this article.

All properly designed engineering structures carry extra margin as a safeguard against failure, owing to the statistical nature of imposed loads and material properties. Such design margins are well established for most space/aircraft structures; the frequently quoted factors of safety for ultimate and yield strengths are mature and generally well understood. Unfortunately, the established design factors may not apply to the unique structure of the thin-layered sunshield.

Addressing the need to establish design bounds and evaluate the error budget, we instituted a comprehensive program of membrane testing. Detailed in the following section, the program examines the effect of gravity, seams, deviations due to manufacturing operations, and other factors. It also answers a basic question: Given a simple geometry and known edge conditions, is it possible to accurately predict wrinkles, as well as the global response? The test has conclusively demonstrated that it is indeed possible to predict both with a high degree of accuracy, if the initial shape or state of a membrane is available.

Therefore, precise measurement and detailed knowledge of the as-built shape of the sunshield will be vital to reliable verification of its expected performance. ManTech SRS Technologies, Inc., will manufacture the membrane of the sunshield, as well as conduct design and analysis of the sunshield in parallel with the Northrop Grumman/JWST structure group activities, described previously. Our two-team approach facilitates independent review and cross-checking of the complex design and analyses.

The current verification plan calls for measuring the sunshield's as-built shape with the help of a light detection and ranging system (lidar), a laser-based optical instrument discussed below (page 32). The sunshield will be surveyed in the horizontal position while supported by loading fixtures. The effect of gravity will significantly alter the membrane shape to which the sunshield has been designed. We expect deep wrinkles and sag of a few inches. Further, we anticipate that the assembled sunshield will have already deviated from its membrane shape, owing to errors in the assembly process.

Under those conditions, a simple comparison between the simulated membrane shape loaded under gravity and the measured sunshield shape may produce misleading results, as the process involved is highly nonlinear. Possible methods are being examined to mathematically compute the gravity-loaded as-built shape. They include taking measurements of the as-built sunshield under gravity and using that information to analytically unload the model in order to predict its on-orbit shape. Unfortunately, analysis of the sunshield in the almost unloaded state is extremely difficult. The problem: membrane tension acts as a solution stabilizer, and, if the sunshield or a part becomes slack, the solution process becomes exponentially unstable. To overcome the numerical complications, additional solution methods are currently being explored.

Test Program for James Webb Space Telescope Sunshield

The membrane analysis correlation test plan uses a multiphase approach of increasing complexity:

- *Test 1* was designed to demonstrate an ability to predict wrinkles, given a membrane with precisely known, applied membrane forces.
- *Test 2* was designed to determine the degree of accuracy to which wrinkles can be predicted for a membrane with flightlike features, such as seams, compliant borders, and catenary-induced loading.

Further descriptions of the components are included in the following subsections. Additional tests will evaluate the effects of other flightlike components of the sunshield design, as well as quantify the uncertainties related to manufacturing.

Tests 1 and 2 both

- Use loading conditions derived to load the membrane such that the central surface is flat, in order to inspect the as-built condition.
- Produce wrinkles of varying wavelength and amplitude across the center of the test article. Controlling the wrinkle patterns allows

  - Minimization of wrinkles on the perimeter of the membrane
  - Creation of wrinkles of a discernible amplitude

When those criteria are met, two benefits accrue:

- The physics of the problem are demonstrated to be well understood.
- The test results can be assessed both qualitatively and quantitatively.

A simple visual inspection would determine whether the test results were reasonably close to analytically predicted results. It may also be possible that the ability to control the direction and location of wrinkles can be used as an additional mechanism to satisfy thermal requirements on the cold-side membrane.

Test Articles. Test 1 used a 48.0 × 48.0 in. (121.9 × 121.9 cm) test article. The membrane was constructed of 1.0-mil (25.4-μm) Kapton, with a single-sided vapor-deposited aluminum coating (see Figure 11). The test article has seven attach points at each of the four sides, reinforced using glass fiber doublers. To load the membrane to a near-flat condition, the load case chosen is the inverse of the load generated by the test article sagging under gravity. That load case is the initial, as-built condition used to verify the quality of the membrane material. Other load cases are generated by superimposing additional concentrated loads near the center of one side of the test article. Two load cases for measuring wrinkle patterns may be obtained by increasing the load at three of the center attach points by 2.0 lbf, then 3.0 lbf.

Test 2 employed three articles:

- A 48.0 × 48.0 in. (121.9 × 121.9 cm) membrane with no seams, loaded by an external catenary
- A 48.0 × 48.0 in. membrane with a single welded seam, also loaded by an external catenary
- A 100.0 × 100.0 in. (254 cm × 254 cm) membrane with two welded seams, loaded by an internal catenary that is implemented together with a compliant border

The 48-in. test articles both use scalloped edges with reinforced attach points. Metal c-clips are employed as standoffs to a high-strength catenary cable, as Figure 12 shows. The catenary shape, modeled using a high-order polynomial equation, is designed to transmit load into the membrane in a manner similar to the initial-shape condition of Test 1. To provide for measurable wrinkles at the center region, a deeper catenary section is superimposed on the first test article (Figure 12a) to increase the load in a specific region. The second test article in Test 2 is exactly the same as the first, except for a thermally lap-welded seam running parallel to the wrinkle direction (Figure 12b).

Figure 13 shows a detailed view of the seam, a process developed by ManTech SRS. Two segments of membrane material are placed over each other to form a lap joint. The thermal process bonds the membranes together using a pattern resembling a spot weld. One challenge of the analysis is to determine how well thermal welds can be characterized, as they may affect the global or local membrane response.

The third and final test article in Test 2 uses a specimen with a larger membrane, but the same catenary geometry, as Figure 14 shows. Due to the nature of the internal catenary—a stainless-steel band bonded to the outer edge of the membrane—the load-introduction points must be reinforced. Grommets are used at the end points of the catenaries, along with local Kapton doublers to increase strength and prevent tearing. The test article uses two seams running perpendicular to the wrinkle direction.

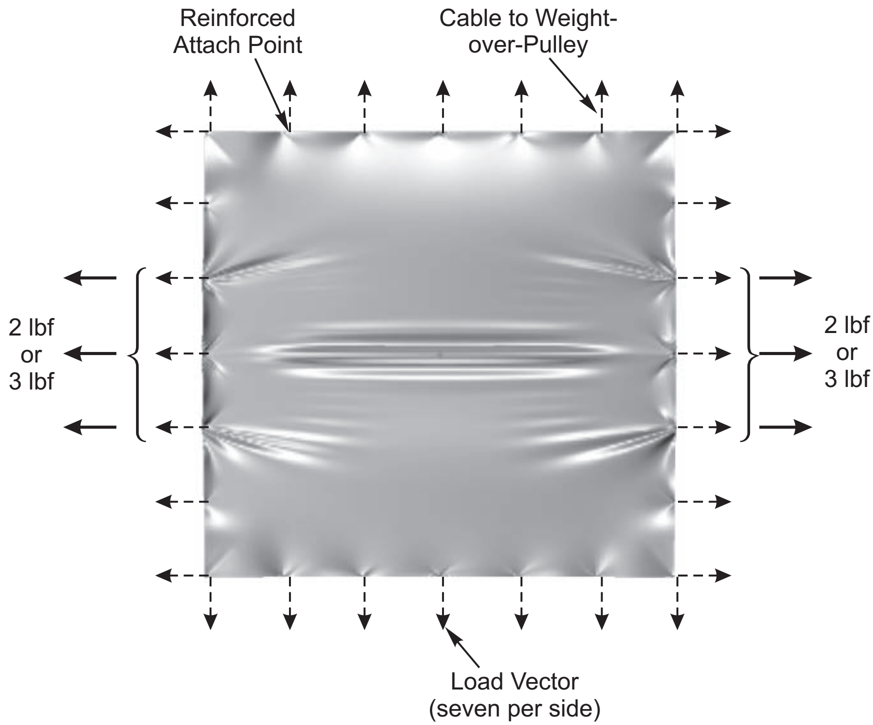

Figure 11. Test 1: 48-in. membrane

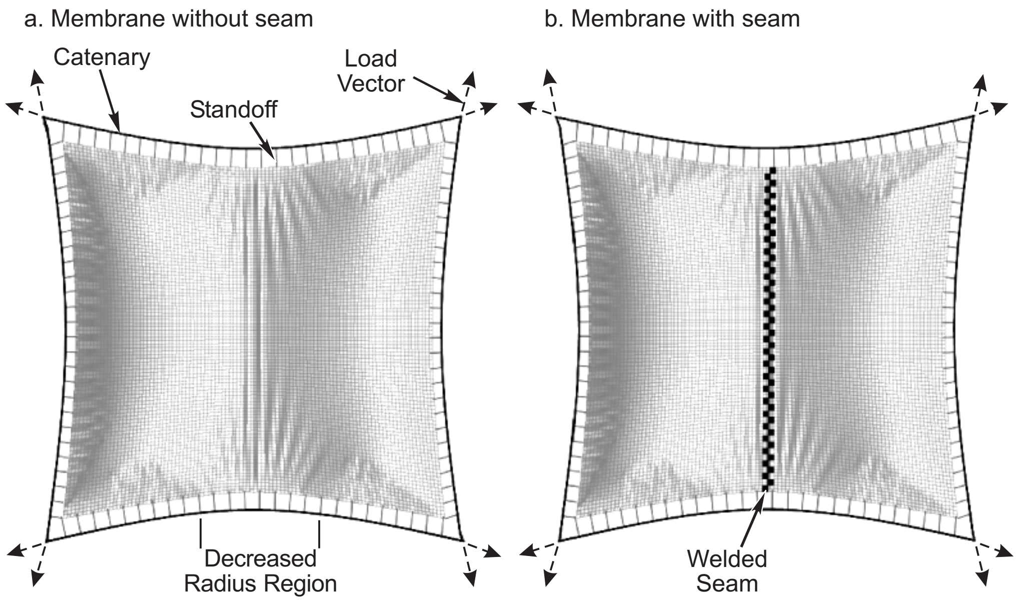

Figure 12. Test 2: 48-in. membrane with and without seam

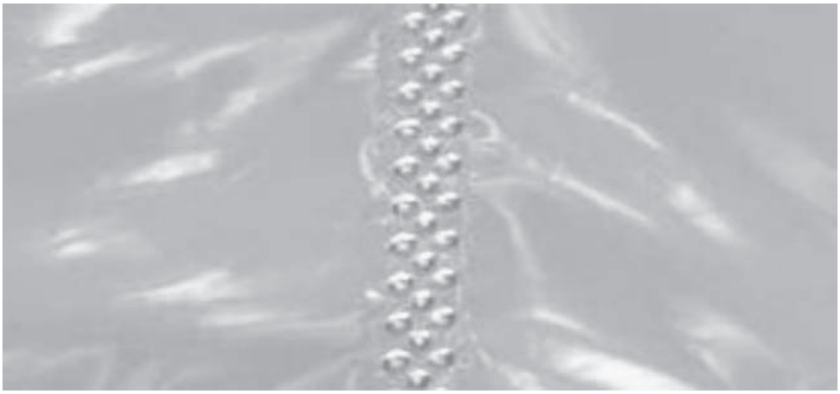

Figure 13. Thermally lap-welded seam

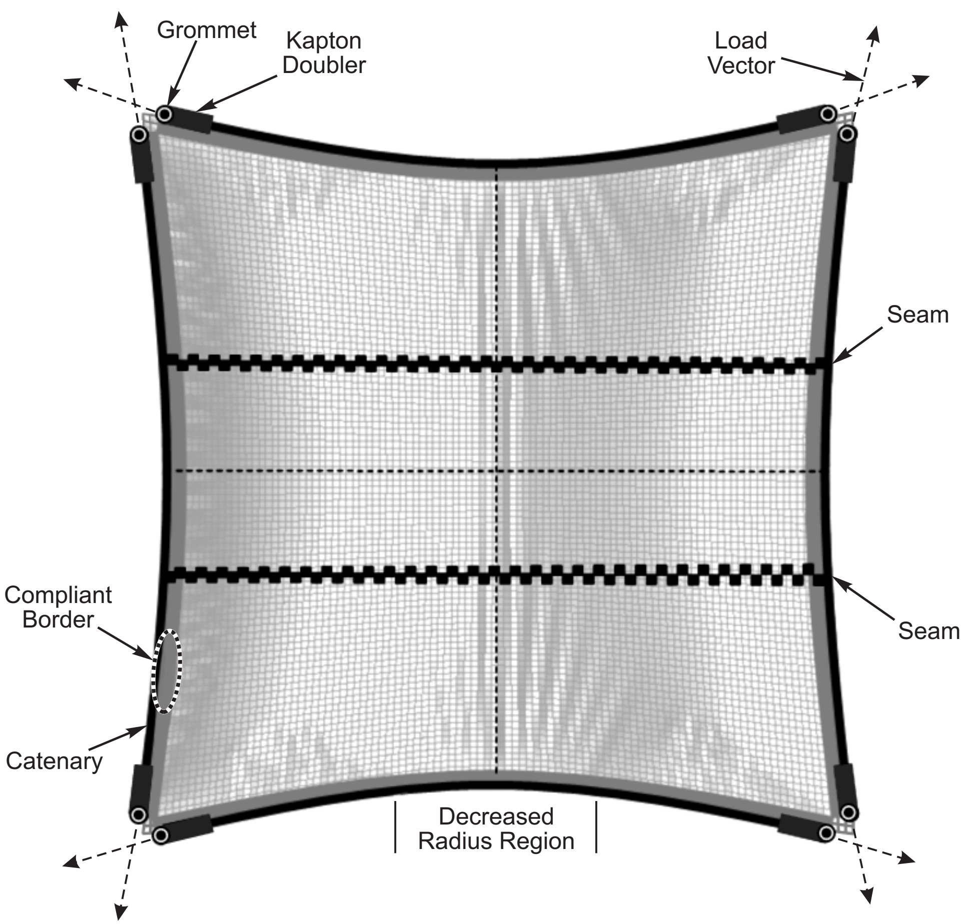

Figure 14. Test 2: 100-in. membrane with seams, internal catenary, and compliant border

The compliant border, another development of ManTech SRS, is used in conjunction with an internal catenary [7]. Illustrated in Figure 15, the compliant border allows a tension load application into the catenary cables, while minimizing or eliminating the shear load induced into the membrane. Such a border is necessary at the corners, where the load is introduced. The compliant border is produced by a thermal forming process that creates a series of parallel pockets. The local elongation of the material into the pockets allows for a shearing action, while maintaining the ability to place a load into the membrane. Previous work in modeling compliant borders has focused on using a series of rod (truss) elements to model the border characteristics [8]. The same technique has been implemented in the FEMs representing this test article.

Test Fixtures and Configurations. Multiple test fixtures are used to support and load the test articles; one such test fixture is shown in Figure 16. The fixtures are designed for dimensional stability and earthquake safety. They are also designed to be placed in both a horizontal and a vertical configuration. A weight-over-pulley system is used to load the test articles and allow for changes in orientation.

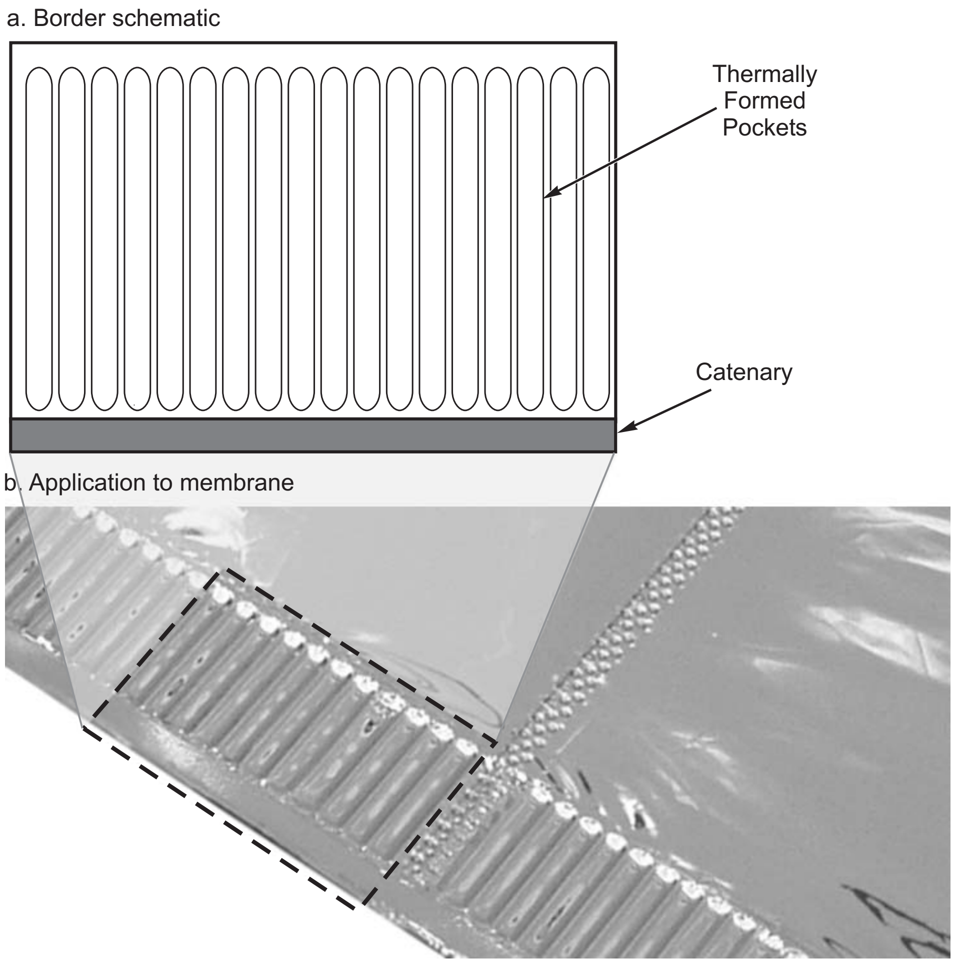

Figure 15. Compliant border schematic and application to 100-in. membrane

a. Horizontal test fixture b. Vertical test fixture

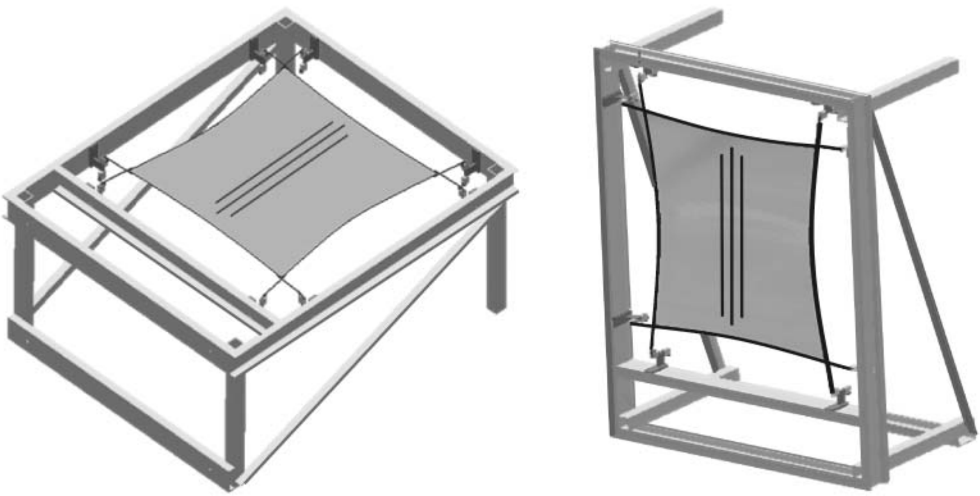

Figure 16. Test fixture: Horizontal and vertical orientations

Measurement System. To measure the surface of the test articles, we chose a lidar—a light imaging detection and ranging system, shown in Figure 17. Similar in principle to radar systems, lidar uses laser light (instead of radio waves) when measuring the time delay between transmission and detection of a reflected signal. The lidar system allows for the accurate measurement of the membrane test articles, while not requiring the application of retroreflective adhesive targets, as commonly required by photogrammetric techniques. Dot-projection photogrammetry—a technique where projected dots of light are used as targets—was investigated but found not able to provide the measurement resolution desired. The unit used for these experiments was a Metris MV224 lidar system.

Results and Discussion

In the following review of Tests 1 and 2, we focus on correlation between test results and finite element modeling.

Test 1 Results: 48-in. Membrane, 2-lbf and 3-lbf loads. Case 1 examined an application of an additional 2-lbf load. Figure 18a shows a photograph of the test article; Figure 18b shows the FEM deflection results. Visual inspection finds excellent correlation in the membrane response. The figure shows a significant center wrinkle and a set of wrinkles on the fringes that do not cross the length of the membrane. A slight deviation exists between the physical test response to the load at the edges of the membrane and the analytical FEM results because the load introduction points are difficult to characterize.

Case 2 is the application of an additional 3-lbf load. Figure 19 shows a photograph of the test article on the left and the FEM deflection results on the right. Again, visual inspection shows excellent correlation between the test article's response and the FEM deflection results. Three large wrinkles run across the membrane. The same minor deviations occur at the membrane boundary.

Figure 20 compares, for both load cases, the lidar measurements with the FEM's deflection results through the center of the membrane. Correlation for both load cases is quite good;

a. Metris MV224 lidar system

b. Lidar measuring test article

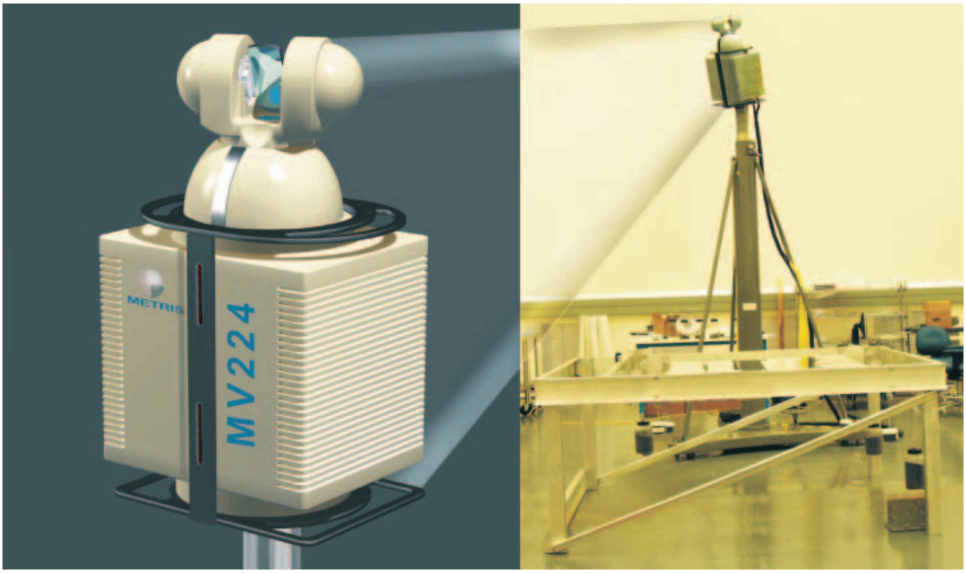

Figure 17. Metris MV224 lidar system used to measure 48-in. test article

a. 2-lbf-load test article results

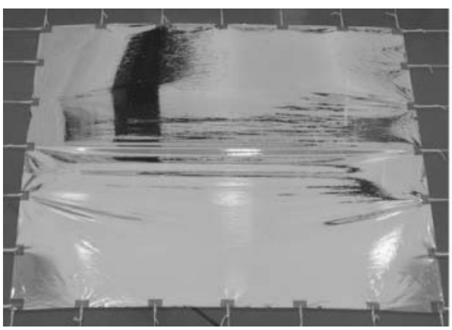

b. Finite element modeling deflection results

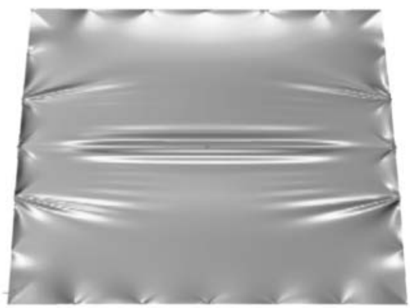

Figure 18. 48-in. membrane with 2-lbf load: Test article results and finite element modeling deflection results

a. 3-lbf load test article results

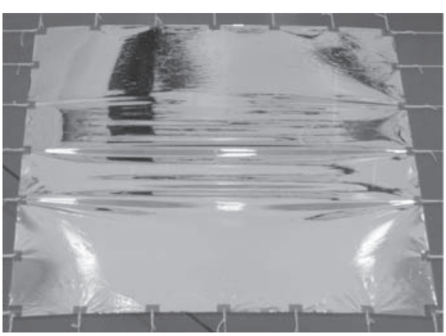

b. Finite element modeling deflection results

Figure 19. 48-in. membrane with 3-lbf load: Test article results and finite element modeling deflection results

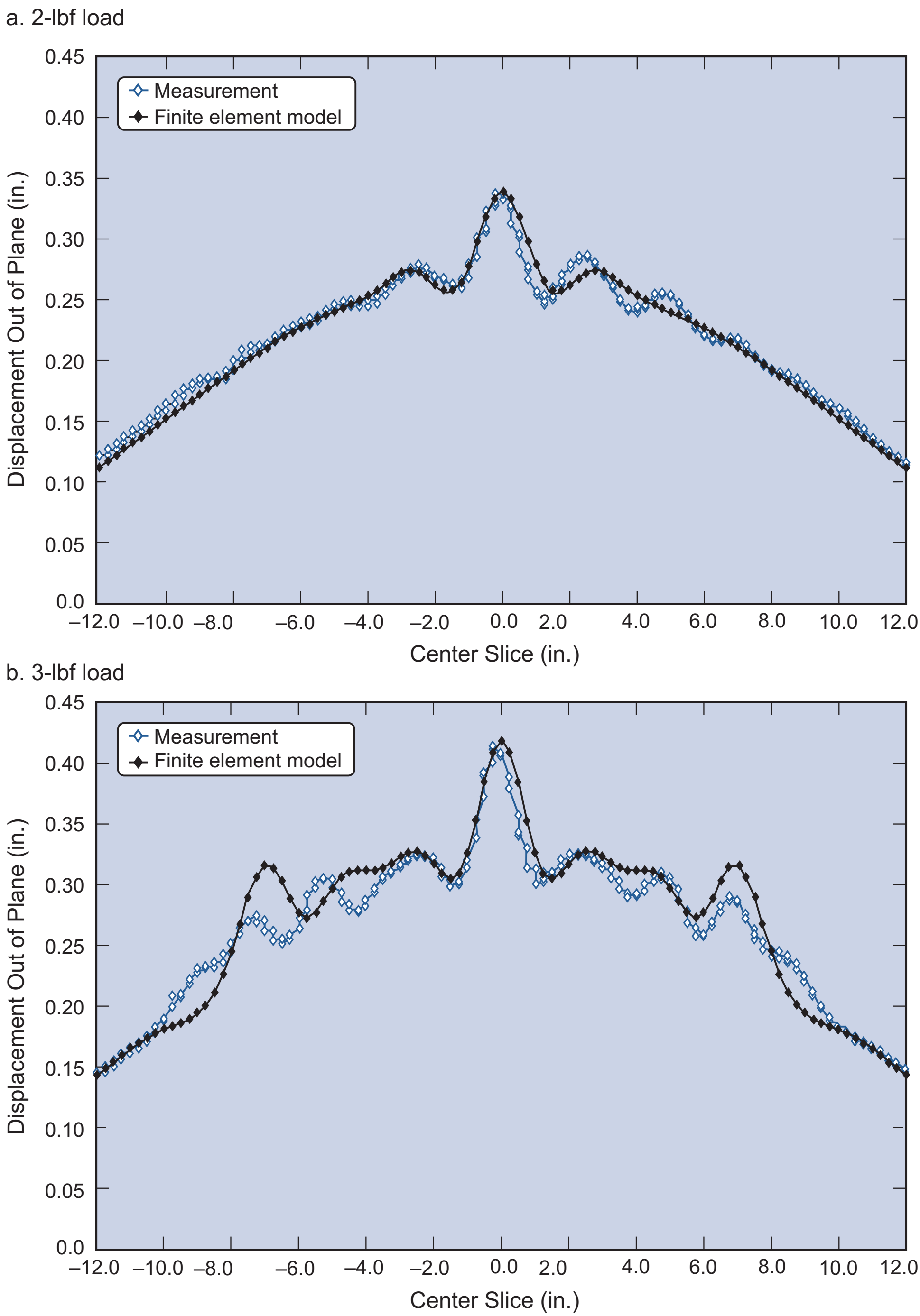

Figure 20. Measurement compared with finite element model: Test 1, 2-lbf and 3-lbf loads

the central wave amplitudes match very well. Deviations exist in the remainder of the wave pattern, possibly due to material imperfections.

Table 1 compares the maximum amplitude and wavelength computed by test and by analysis. Multiple samples were taken for test articles and the results are given as statistical quantities. The maximum amplitude correlates extremely well. The wavelength shows an overprediction of 20%. In fact, the lidar data sample used for this test was insufficient, so a ±0.25-in. measurement tolerance exists. This tolerance accounts for the deviation shown in the data, which is not apparent from the plots shown previously. Overall, for test articles with accurately known point input loads, correlation with FEM results has been excellent.

Test 2 Results: 48-in. Membrane, No Seam. The first case in Test 2 is the 48-in. membrane with an application of 25 lbf in the catenary with the small radius section and a 2.5-lbf load in the other. Figure 21 shows a photograph of the test article on the left and the FEM results on the right. Visual inspection shows good correlation in the test article's response, compared with that of the FEM. Three large wrinkles running across the membrane can be observed in both the test article and the FEM.

The second case in Test 2 is the same 48-in. membrane with an application of 25 lbf in the catenary with the small radius section and a 3.75-lbf load in the other. Figure 22 shows a photograph of the test article on the left and the FEM results on the right. A similar good correlation in the test article's response is found, with three large wrinkles crossing the membrane.

Figure 23 compares, for both load cases, the lidar measurements with the FEM's deflection results through the center of the membrane. Correlation for the two load cases is good, with an accurate wavelength and wrinkle amplitude. Overall, the global shape is predicted accurately. Deviation is minor, on the order of mils, as the measurements approach the membrane boundaries. The photographs of the test articles do show some additional wrinkling, which may be due to material imperfections. Additionally, the 3.75-lbf example shows small wrinkles that are not accounted for by the model. The membrane material may be exhibiting some creep after repeated load cycles, as these were some of the final samples for this test article.

Table 1. Computed results for maximum amplitude and wavelength: Test 1, 2-lbf and 3-lbf loads

Case	Maximum Amplitude (in.)	Wavelength (in.)
Case 1: 2-lbf load		
Finite element model	0.081	3.00
Mean of test samples	0.082	2.50
Standard deviation of test samples	0.020	0.00
Test versus finite element model (% difference)	–1.22%	20.0%
Case 2: 3-lbf load		
Finite element model	0.118	3.00
Mean of test samples	0.118	2.50
Standard deviation of test samples	0.016	0.00
Test versus finite element model (% difference)	–0.43%	20.0%

a. Test article results

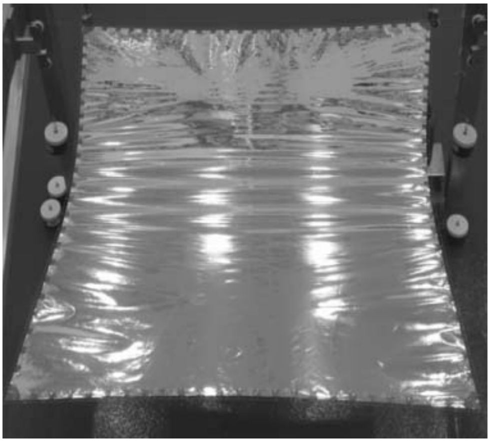

b. Finite element modeling deflection results

Figure 21. 48-in. membrane, no seam, 25 × 2.5 lbf load: Test article results and finite element modeling deflection results

a. Test article results

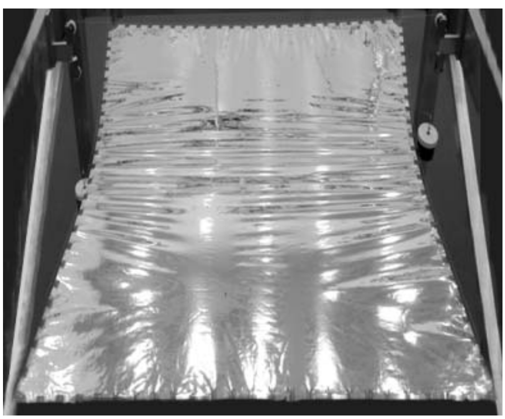

b. Finite element modeling deflection results

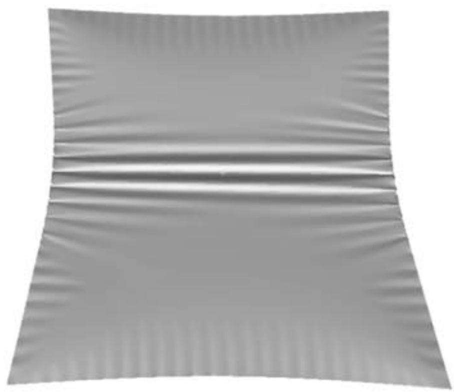

Figure 22. 48-in. membrane, no seam, 25 × 3.75 lbf load: Test article results and finite element modeling deflection results

Table 2 compares the maximum amplitude and wavelength computed between test and analysis. Again, multiple samples were taken for both test articles; the results are thus given as statistical quantities. The maximum amplitude and slopes are predicted between 1% and 26%, quite good in any test correlation. In addition to the more complex loading condition, other factors increase the difficulty of tests using an external catenary. The catenaries have a certain amount of friction between the cables and standoffs. Additionally, we determined analytically that the manufacturing tolerances on the catenary geometry are much more sensitive to minor pullout on the attach points. We also identified an operating region for the test articles using external catenaries. If the applied load were too low, friction would dominate; if too high, manufacturing tolerances would become more evident, with particular areas witnessing concentrated loads.

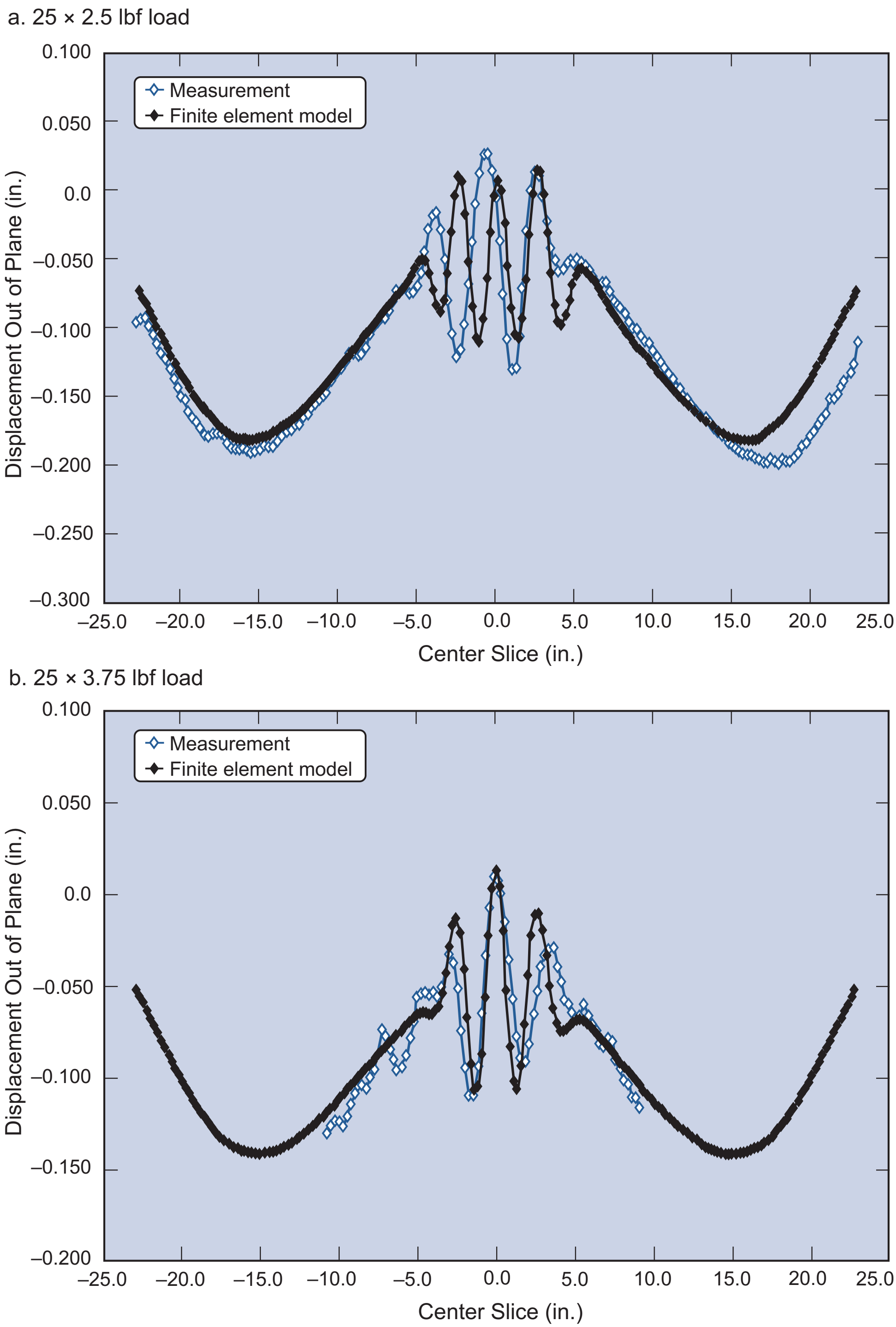

Figure 23. Measurement compared with finite element model: Test 2, 48-in. membrane, 25 × 2.5 lbf and 25 × 3.75 lbf loads

Table 2. Computed results for maximum amplitude and wavelength: Test 2, 48-in. membrane, no seam, 25 × 2.5 lbf and 25 × 3.75 lbf loads

Case	Maximum Amplitude (in.)	Wavelength (in.)
Case 1: 25 × 2.5 lbf load		
Finite element model	0.123	0.150
Mean of test samples	0.155	0.151
Standard deviation of test samples	0.029	0.026
Test versus finite element model (% difference)	–26.3%	–0.9%
Case 2: 25 × 3.75 lbf load		
Finite element model	0.122	0.147
Mean of test samples	0.115	1.22
Standard deviation of test samples	0.037	0.036
Test versus finite element model (% difference)	4.8%	17.0%

Test 2 Results: 48-in. Membrane with Seam. The next two load cases use the seamed 48-in. test article. Currently, that thermal seam is modeled by thickening the shell (plate) elements in the corresponding region of the seam. The third case in Test 2 is the 48-in. seamed membrane with an application of 25 lbf in the catenary with the small radius section, and a 2.5-lbf load in the other (similar to Test 2, Case 1). Figure 24 presents a photograph of the test article and the FEM analytical results. Visual inspection shows reasonable correlation between the test article's response and the FEM results, despite a flat region attributed to the residual stress in the seam and currently not captured by the analysis.

The fourth case in Test 2 is the 48-in. seamed membrane with an application of 25 lbf in the catenary with the small radius section, and a 3.75-lbf load in the other (similar to Test 2, Case 2). Figure 25 presents a photograph of the test article on the left and the FEM results on the right. Again, visual inspection shows a reasonable correlation between the test article's response and that of the FEM, despite, again, a flattened region.

Figure 26 compares, for both load cases, the lidar measurements with the FEM's deflection results through the center of the membrane. An interesting result of the seam is that the wrinkles in the immediate area are flattened (highlighted on the plot). Overall, the global shape is still predicted accurately, and wrinkles in the area surrounding the flattened section are captured. The seam influences the wrinkling in the immediate area (highlighted on the plot). Overall, the global shape is predicted accurately and wrinkles in the area surrounding the flattened section are captured. The typical minor deviations appear near the boundaries of the test article.

Table 3 compares the maximum amplitude and wavelength computed between test and analysis. The maximum amplitude and slopes are predicted on roughly the same order as for the nonseamed test article. The seams significantly influence the local response.

Finally, a diagonal-load case was attempted where a 9.0-lbf load was applied to two corners. Figure 27 compares the test article with the FEM results. Overall, visual correlation is quite good, though deviations result from the interaction with the seams. Unexpectedly, the wrinkle pattern of the test article is not completely symmetric. On the left side, the wrinkles do not extend as far as on the right side, likely being attenuated by the seams. The results of these three tests provide more confidence in the analytical techniques, although they show the necessity of additional study in the modeling of seams.

a. Test article results

b. Finite element modeling deflection results

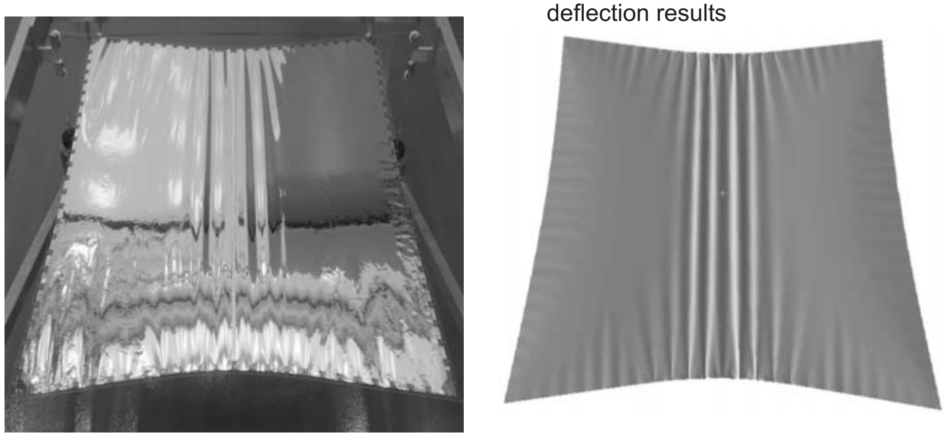

Figure 24. 48-in. membrane with seam, 25 × 2.5 lbf load: Test article results and finite element modeling deflection results

a. Test article results

b. Finite element modeling deflection results

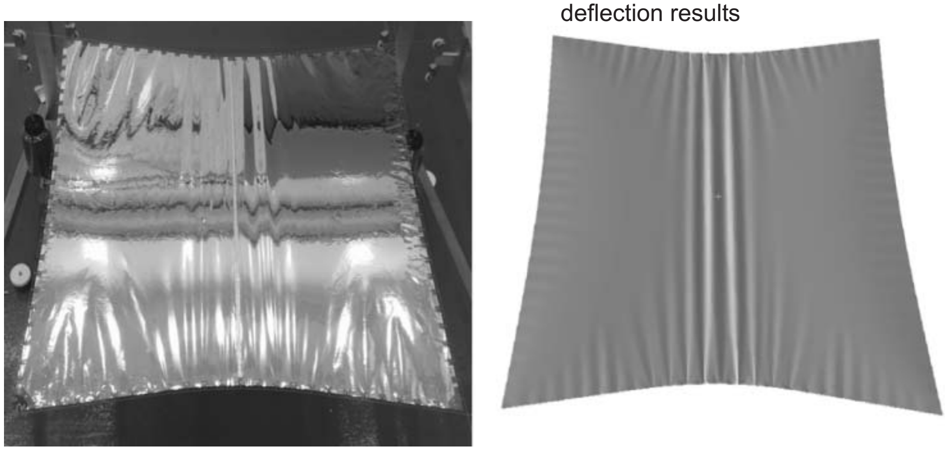

Figure 25. 48-in. membrane with seam, 25 × 3.75 lbf load: Test article results and finite element modeling deflection results

Test 2 Results: 100-in. Membrane. The final study in Test 2 uses the 100-in. test article, a membrane of larger size and greater complexity (using additional flight hardware). This test case loads the membrane with 50 lbf in the catenary with the small radius section, and a 7.5-lbf load in the other (similar to Test 2, Cases 2 and 4, but with double the load).

Figure 28 presents a photograph of the test article on the left and the FEM results on the right. Visual inspection shows a lack of correlation between the test article's response and that of the FEM. The major wrinkle predicted through the center of the membrane does not exist. Significant wrinkling, more than was predicted, occurs at the corners.

Figure 29 compares the lidar measurements with the FEM's deflection results through the center of the membrane. The lidar measurements show the lack of wrinkles through the center of the membrane. However, the global shape is predicted accurately. The large wrinkles at the corner likely signify that the compliant border width chosen for this test

a. 25 × 2.5 lbf load

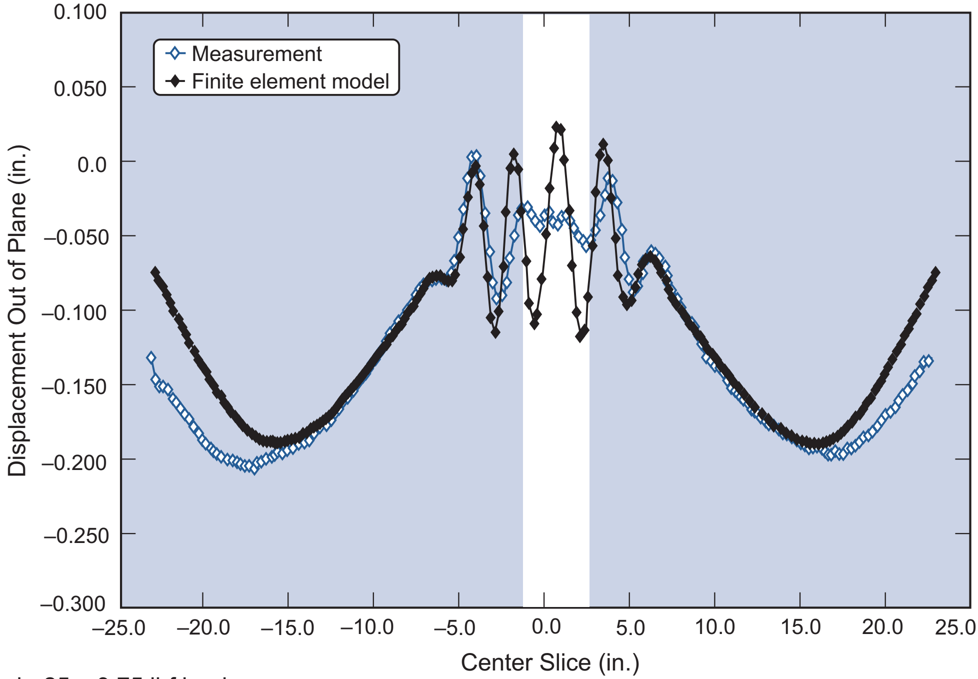

b. 25 × 3.75 lbf load

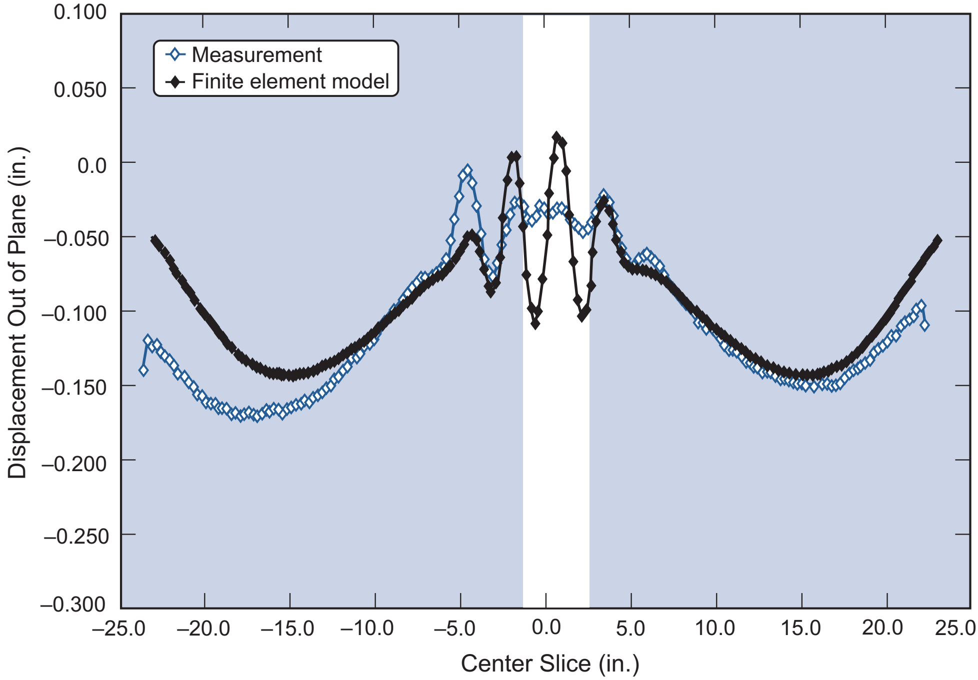

Figure 26. Measurement compared with finite element model: Test 2, 48-in. seamed membrane, 25 × 2.5 lbf and 25 × 3.75 lbf loads

Table 3. Computed results for maximum amplitude and wavelength: Test 2, 48-in. seamed membrane, 25 × 2.5 lbf and 25 × 3.75 lbf loads

Case	Maximum Amplitude (in.)	Wavelength (in.)
Case 3: 25 × 2.5 lbf load		
Finite element model	0.141	0.165
Mean of test samples	0.147	0.159
Standard deviation of test samples	0.034	0.033
Test versus finite element model (% difference)	–4.5%	3.8%
Case 4: 25 × 3.75 lbf load		
Finite element model	0.125	0.141
Mean of test samples	0.087	0.084
Standard deviation of test samples	0.010	0.016
Test versus finite element model (% difference)	30.3%	40.6%

a.Test article results

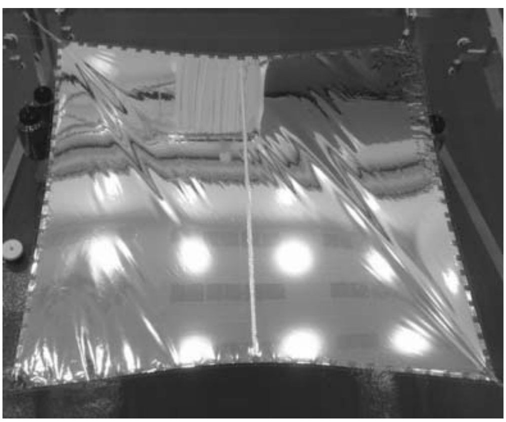

b. Finite element modeling deflection results

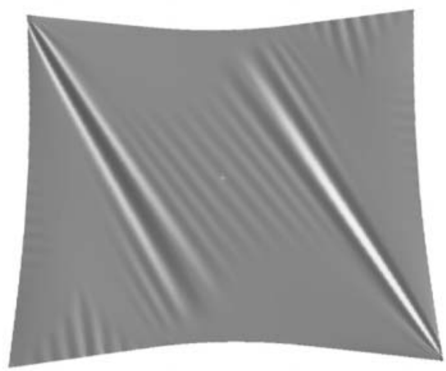

Figure 27. 25 × 2.5 × 9 lbf diagonal load: Test article results and finite element modeling deflection results

a. Test article results

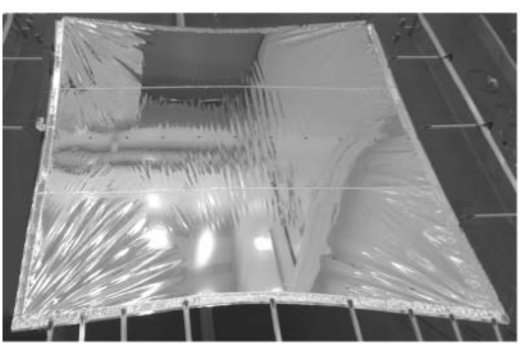

b. Finite element modeling deflection results

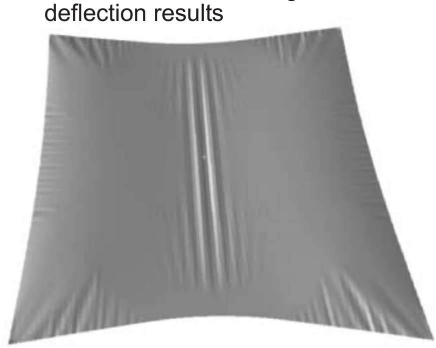

Figure 28. 100-in. membrane with 50 × 7.5 lbf load: Test article results and finite element modeling deflection results

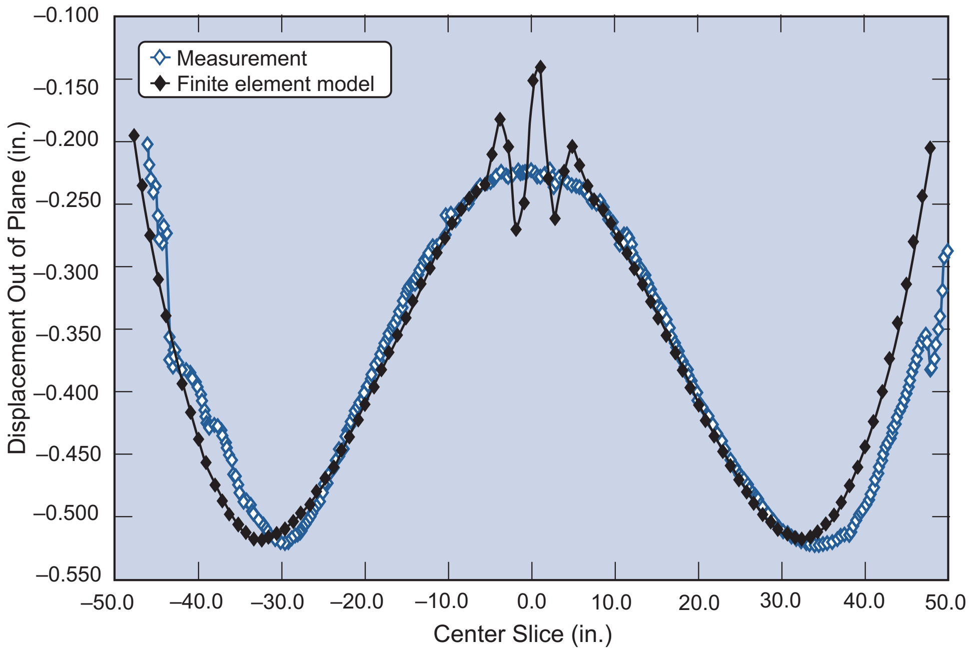

Figure 29. Measurement compared with finite element model: Test 2, 100-in. membrane, 50 × 7.5 lbf load

specimen was insufficient, or that the characterization of the border using an idealized model is not accurate. Further study into how to characterize the compliant border will be necessary to more accurately model this membrane. An additional issue with this larger membrane is its increasing sensitivity to manufacturing tolerances.

Figure 30 examines the 100-in. as-built membrane with loading added to achieve a flat surface. The photo on the left shows an area of wrinkling, where the membrane should be absolutely flat. Closer inspection shows a region with wrinkling, signifying compression—more evidence of material imperfections that can exist in Kapton E, owing to the method of manufacture. Rolls of the material are cooled over large rollers, which likely cause local regions of material elongation and yield. Signs of puckering are evident in the region near one of the seams. Even though the thermal seaming process is of very high quality overall, it is still subject to alignment and material imperfections. These may be random imperfections that should be analyzed through appropriate uncertainty factors.

Conclusions and Remaining Challenges

Northrop Grumman Space Technology has made substantial progress in the analysis of gossamer structures. We have made significant advances in understanding the physics of membranes, along with issues that arise when manufacturing and testing such structures. Tools have been developed for the analysis of gossamer structures and implemented as part of methodologies derived to optimize the shape of the sunshield. Additionally, those tools have been (and continue to be) subjected to a series of tests to verify model-to-hardware correlation and to aid in further understanding the mechanics of membranes.

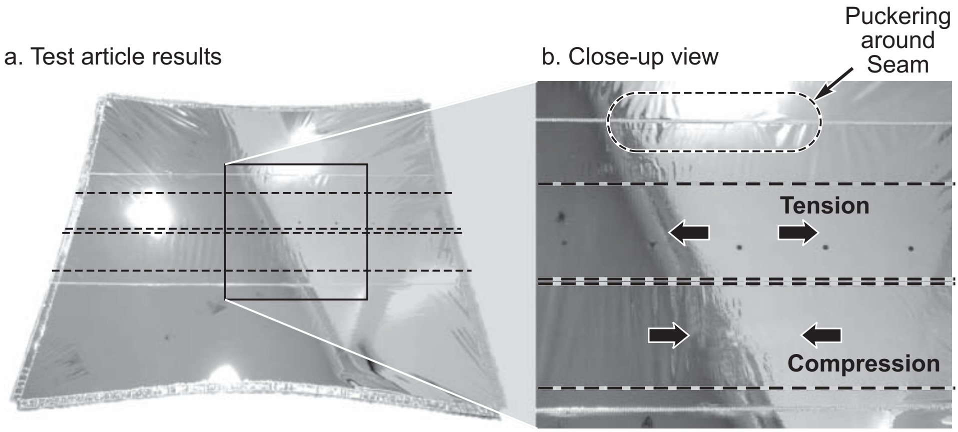

Figure 30. 100-in. membrane with material and seam imperfections: Test article results

Planned work includes research in modeling seams, as welded seams demand more sophisticated characterization. Analytical and/or numerical methods that capture the response of compliant borders will significantly improve our finite element modeling. As the sunshield subsystem moves toward Preliminary Design Review in early 2008 and Critical Design Review thereafter, the development of methodologies to accurately determine the as-built shape of a membrane is vital, because precise measurement of large-scale gossamer flight articles in a zero-gravity environment is not possible.

Acknowledgments

The project was funded by the National Aeronautics and Space Administration, whose support is gratefully acknowledged. The authors wish to thank Kevin S. Sewell of Northrop Grumman Space Technology for identifying and implementing the measurement system. Special thanks to sunshield subcontractor ManTech SRS Technologies, Inc., for constructing the membrane test articles and David M. Hedges of Northrop Grumman Space Technology for the design and construction of the test hardware.

References

1. J. Nella, P. Atcheson, C. Atkinson, D. Au, M. Blair, A. Bronowicki, D. Fitzgerald, J. Heidenga, P. Lightsey, T. Kelly, G. Matthews, J. Pohner, P. Reynolds, D. Shuckstes, S. Texter, D. Waldie, and R. Whitley, *Next Generation Space Telescope (NGST) Observatory Architecture and Performance,* Space Telescope Science Institute, November 2002, *http://www.stsci.edu/jwst/trw-spie.pdf*.
2. D.D. Waldie and L.N. Gilman, "Technology Development for Large Deployable Sunshield to Achieve Cryogenic Environment," *Proc. Space 2004 Conference and Exposition*, Paper AIAA-2004-5987, San Diego, California, September 28–30, 2004.
3. C.H. Jenkins, F. Haugen, and W.H. Spicher, "Experimental Measurement of Wrinkling in Membranes undergoing Planar Deformation," *Experimental Mech.*, Vol. 38, No. 2, June 1998, pp.147–152.

4. Y.W. Wong and S. Pellegrino, "Wrinkled Membranes, Part iii: Numerical Simulations," *J. Mech. Materials and Structures*, Vol. 1, No. 1, January 2006, pp. 61–93.
5. C.H.M. Jenkins (ed.), *Gossamer Spacecraft: Membrane and Inflatable Structures Technology for Space Applications, Vol. 191, Progress in Astronautics and Aeronautics*, American Institute of Aeronautics and Astronautics, Reston, Virginia, April 2001.
6. C.H.M. Jenkins (ed.), *Recent Advances in Gossamer Spacecraft, Vol. 212, Progress in Astronautics and Aeronautics*, American Institute of Aeronautics and Astronautics, Reston, Virginia, January 2006.
7. C. Talley,W. Clayton, P. Gierow, J. McGee, and J. Moore, "Advanced Membrane Materials for Improved Solar Sail Capabilities," *Proc. 43rd Conf. AIAA/ASME/ ASCE/AHS/ASC Structures, Structural Dynamics, and Materials: Third AIAA Gossamer Spacecraft Forum*, Paper AIAA-2002-1561, Denver, Colorado, April 22–25, 2002.
8. J. Leifer, "Simplified Computational Models for Shear-Compliant Borders in Solar Sail," *J. Spacecraft and Rockets*, Vol. 44, No. 3, May/June 2007, pp. 571–581.

Author Profiles

Ryan A. Fellini, an engineer at Northrop Grumman Space Technology, currently supports the JWST sunshield integrated product team. Prior to arriving at Northrop Grumman Space Technology, he worked for a year at Ford Motor Company developing optimization software. His research interests include mathematical optimization, design under uncertainty, spacecraft systems, and structures. Dr. Fellini holds a BS in mechanical engineering from the Virginia Polytechnic Institute and State University in Blacksburg, Virginia, as well as an MS and a PhD in mechanical engineering from the University of Michigan, Ann Arbor.

ryan.fellini@ngc.com

Yury L. Kropp, an engineer at Northrop Grumman Space Technology, currently supports the JWST sunshield integrated product team. His 25 years of experience include work in the nuclear energy, aircraft, and spacecraft industries. Along with his knowledge of structural engineering, analysis, and design of composites, he possesses significant experience in the field of nonlinear finite element methods. Mr. Kropp holds both a BS and an MS in mechanical engineering from the University of California, San Diego.

yury.kropp@ngc.com